THE BULLETIN OF OKAYAMA UNIVERSITY OF SCIENCE No. 53 A pp. 31-40(2017)

Electrical and magnetic properties of layered selenide $Tl(Cu_{1-x}M_x)_2Se_2$ (M = Mn, Fe, Co, Ni, Ag)

Tsukio Ohtani, Tomohiro Morinaga*, Shinsuke Namba*, and Satoshi Nakai*

Laboratory for Solid State Chemistry, Department of Chemistry, Faculty of Science,
**Graduate School of Science,*
Okayama University of Science,
Ridai-cho 1-1, Kita-ku, Okayama 700-0005, Japan
(Received October 12, 2017; accepted December 4, 2017)

Physical properties of $Tl(Cu_{1-x}M_x)_2Se_2$ (M = Mn, Fe, Co, Ni, Ag) were investigated. a) $Tl(Cu_{1-x}Mn_x)_2Se_2$ showed the single phase region with $ThCr_2Si_2$-type structure in the composition range of $x \leq 0.40$. All samples showed metallic conduction and ferromagnetism (Curie temperature $T_c = \sim 100$ K). b) $Tl(Cu_{1-x}Fe_x)_2Se_2$ ($0 \leq x \leq 1$) samples showed basically the $ThCr_2Si_2$-type structure. A new phase with modified $ThCr_2Si_2$-type structure was found in the sample of $x = 0.05$. Metallic conduction was observed in the samples of $x \leq 0.20$, and semiconductive conduction for $x \geq 0.30$. Seebeck measurements of these samples revealed that the dominant carriers are holes for $x \leq 0.27$, and are electrons for $x \geq 0.29$. Samples of $x \leq 0.20$ showed Curie temperature T_c at ~ 80 K. c) $Tl(Cu_{1-x}Co_x)_2Se_2$ ($0 \leq x \leq 1$) samples were found to have basically the $ThCr_2Si_2$-type structure. New phases having modified $ThCr_2Si_2$-type structure were found at $x = \sim 0.30$, ~0.60, and ~0.90. All samples showed metallic conductivity. Curie temperature T_c was observed at ~20 K for $x = 0.40$-0.50, and at ~100 K for $x \geq 0.60$. d) $Tl(Cu_{1-x}Ni_x)_2Se_2$ was stable in the range $x \leq 0.10$. All samples showed metallic conduction and diamagnetic behavior. e) $Tl(Cu_{1-x}Ag_x)_2Se_2$ was stable in the range $x \leq 0.10$, and showed quite low resistivity ($\rho = \sim 2 \times 10^{-7}$ Ω.cm) below ~10 K. All the present compounds showed no superconductivity above 2K.

Keywords: $TlCu_2Se_2$; $Tl(Cu_{1-x}M_x)_2Se_2$ (M = Mn, Fe, Co, Ni, Ag); 3d transition elements; layered copper selenide; $ThCr_2Si_2$-type structure; X-ray diffraction; electrical resistivity; metallic conductivity; semiconductor; magnetic susceptibility; ferromagnetism; Curie temperature; Seebeck effect; thermoelectric power factor; electron conduction; hole conduction.

1. Introduction

Ternary copper chalcogenides show a large variety of electrical properties from metallic to semiconductive nature. Folmer and Jellinek found in XPS measurements that the formal oxidation state of copper in most of copper chalcogenides is +1[1]. These observations well explain that ternary copper chalcogenides such as KCu_3S_2[2], KCuS[3], and $BaCu_2S_2$[4,5] have the semiconductive nature due to the filled bands of $3d^{10}$ state of Cu^+, and those such as $TlCu_2X_2$ (X = S, Se, Te)[6-9] and $TlCu_4Se_3$[10] show the metallic nature owing to the hole donation to the energy bands for the charge compensation. The metallic nature was also observed in Cu-deficient ternary copper chalcogenides such as $ACu_{7-x}S_4$ (A = Tl, K, Rb)[11,12], α-, β-$BaCu_{4-x}S_3$[13,14], $TlCu_{3-x}S_2$[15] and $BaCu_{2-x}S_2$[15], which are essentially semiconductive in the stoichiometric compositions.

The schematic crystal structure of $TlCu_2Se_2$ is shown in Fig. 1. The compound adopts $ThCr_2Si_2$-type structure ($I/4mmm$; $Z = 2$) with Cu_2Se_2 layers separated by Tl sheets[7,8]. Each Cu_2Se_2 layer is made of edge-sharing $CuSe_4$ tetrahedra to form anti-PbO type structure. Brun et al. found that $TlCu_2X_2$ (X = Se, Te) shows the metallic behavior with quite low resistivity: $\rho = 8 \times 10^{-6}$ Ω·cm and 6.5×10^{-6} Ω·cm at 77 K for $TlCu_2Se_2$ and $TlCu_2Te_2$, respectively[8]. They claimed that the conductivity is caused by the

mixed-valence state of Tl^{+} and Tl^{3+}. Berger and Van Bruggen[3-9] observed that $TlCu_2Se_2$ is a p-type metal with a Fermi energy of 1.3 eV, and that there is one hole per formula unit in the valence band; the formal valence situation is considered to be $Tl^{+}(Cu^{+})_2(Se_2)^{3-}$.

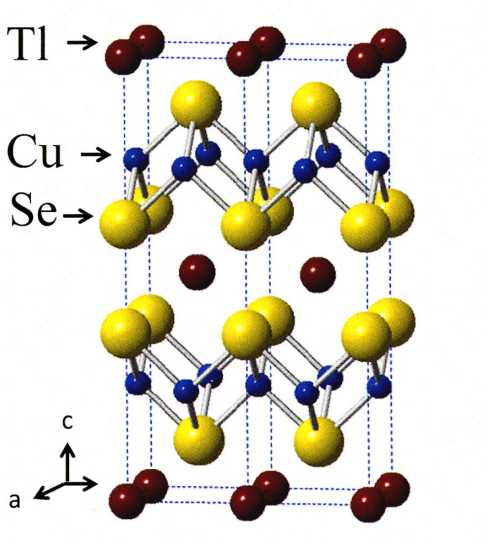

Figure 1. Schematic crystal structure of $TlCu_2Se_2$ ($ThCr_2Si_2$-type structure: $I/4mmm$, Z = 2). The structure consists of Cu_2Se_2 layers separated by Tl sheets.

We have investigated previously the electrical properties of $TlCu_{2-x}X_2$ (X = Se, Te) and $(Tl_{1-x}Ba_x)Cu_2Se_2$ in more detail[16]. We found that the sintered pellets of $TlCu_2Se_2$ shows quite small value of the resistivity ρ at low temperatures ($\rho = 2\times10^{-7}$ $\Omega\cdot$cm at 2K) in spite of the existence of a large number of grain boundaries, impurities, lattice defects, etc. Hall measurements for these compounds showed that the conduction is carried out by the majority of holes, which are produced for the charge compensation, and by a small number of electrons.

It was reported that $Tl(Cu_{1-x}Fe_x)_2Se_2$ ($0 \le x \le 0.50$) samples show the p-type metallic conductivity for $0 < x < 0.25$, and the semiconductive behavior between x = 0.25 and 0.50[17]. Furthermore, the ferromagnetic ordering was observed in these compounds at 50-80 K. These observations presented some questions, i.e. how the physical properties of $TlCu_2Se_2$ will be changed by the substitution of the other 3d transition elements for copper, at what composition of Fe the ferromagnetism will appear, etc. In the present work we investigated the electrical and magnetic properties of $Tl(Cu_{1-x}M_x)_2Se_2$ (M = Mn, Fe, Co, Ni, Ag).

2. Experiments

$Tl(Cu_{1-x}M_x)_2Se_2$ (M = Mn, Fe, Co, Ni, Ag) samples were prepared as follows. The elemental mixtures with desired ratios were sealed in silica tubes in vacuo, and were heated at 773 K for 7 days. Reacted samples were annealed at 523 K for 7 days after palletization, and then were slowly cooled to room temperature. The starting elements were: Tl (Katayama Chemicals, 99.99% in purity), Cu (Wako Pure Chemical Ind., 99.9% in purity), Mn (Wako Pure Chemical Ind., practical grade), Fe (Wako Pure Chemical Ind., 99.9% in purity), Co (Rare metallic Co., Ltd, 99.99% in purity), Ni (Wako Pure Chemical Ind., 99.9% in purity), Ag (Wako Pure Chemical Ind., 99.9% in purity) and Se (Wako Pure Chemical Ind., 99.999% in purity). Elemental Tl was treated in a dry box to avoid the oxidation.

The obtained samples were analyzed by an X-ray diffraction (XRD) method with monochromatic CuKα radiation using a RIGAKU RINT-2500. Electrical resistivity ρ measurements were made on sintered pellets by ordinary dc four probe method from 2.0 to 300 K. Seebeck (S) measurements were performed in the temperature range of 120-300K using Cu leads by keeping a temperature gradient of ~3 K. Magnetic susceptibility χ and magnetization measurements were carried out by using a SQUID magnetometer (Quantum Design: MPMS XL5) from 4K to room temperature (to 700 K for some samples).

3. Results and discussion

3.1. $Tl(Cu_{1-x}Mn_x)_2Se_2$ system

$Tl(Cu_{1-x}Mn_x)_2Se_2$ samples were found to have the $ThCr_2Si_2$-type structure in XRD measurements. Figure 2 gives x dependences of lattice parameters of $Tl(Cu_{1-x}Mn_x)_2Se_2$. In the composition range of $0 \le x \le 0.40$ the curves obey a Vegard's law, indicating Mn atoms are substituted for Cu atoms in this composition range. XRD patterns showed that the samples of $x \ge 0.50$ contain a small amount of MnSe.

Figure 3 shows temperature variations of electrical resistivity ρ of $Tl(Cu_{1-x}Mn_x)_2Se_2$. All samples show the metallic behavior. The values of ρ increase as x increases. The values of Seebeck coefficients S of all samples were about –5 μVK^{-1} at 110 K, and almost linearly increase with temperature up to about +5 μVK^{-1} at 300 K, suggesting that these compounds are typical metals with mixed conduction.

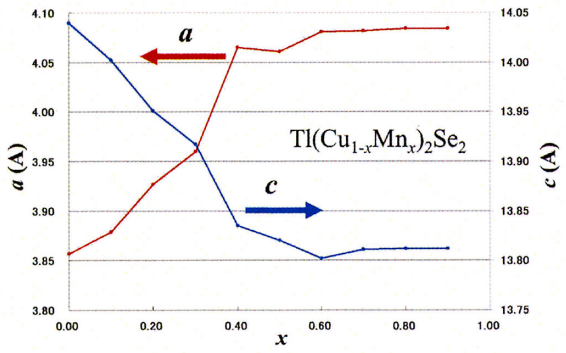

Figure 2. Lattice parameters of $Tl(Cu_{1-x}Mn_x)_2Se_2$ as a function of Mn composition x.

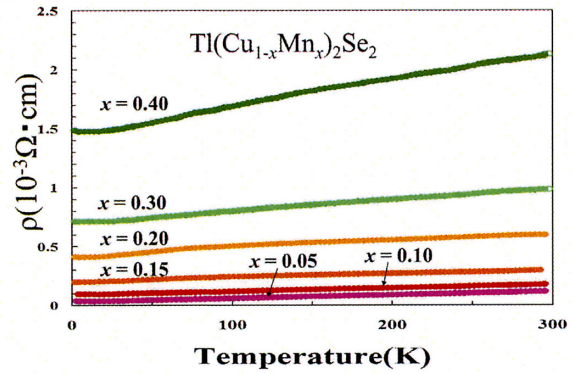

Figure 3. Temperature variations of electrical resistivity ρ of $Tl(Cu_{1-x}Mn_x)_2Se_2$ ($0.05 \le x \le 0.40$).

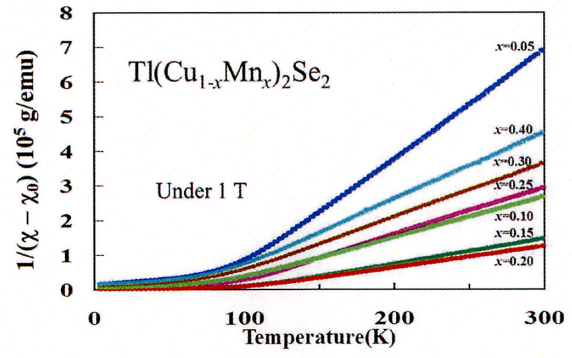

Figure 4. Temperature dependences of inverse magnetic susceptibility $1/(\chi - \chi_0)$ of $Tl(Cu_{1-x}Mn_x)_2Se_2$.

Figure 4 shows temperature variations of inverse magnetic susceptibility of $Tl(Cu_{1-x}Mn_x)_2Se_2$. Above ~ 100 K, magnetic susceptibility χ of all samples obeyed a Curie-Weiss law $\chi = \chi_0 + C/(T - \theta)$, where χ_0, C and θ are a temperature-independent term of χ, a Curie constant, and a Weiss constant, respectively.

Obtained magnetic parameters of these samples are listed in Table I. The ferromagnetic transition was observed for all samples at ~ 100 K, which is consistent with the positive values of Weiss constant θ. In magnetization measurements all samples showed the paramagnetic behaviors at 298 K. The Curie temperature is scarcely varied with x. Although there is no peak of MnSe in XRD patterns, the samples of $0.05 \le x \le 0.40$ may contain MnSe. This selenide is known to be an antiferromagnet[18]. Ferromagnetism, thus, would be intrinsic nature to these compounds. The values of P_{eff} (effective Bohr magneton) were calculated assuming that only Mn ions carry magnetic moments, because Cu^+ ions are in $3d^{10}$ state. The total spin angular momentum S was calculated from the values of P_{eff}.

Table I. Magnetic parameters of $Tl(Cu_{1-x}Mn_x)_2Se_2$. P_{eff} is effective Bohr magneton. θ is Weiss temperature. S is total spin angular momentum.

composition x	χ_0(emu/g)	Peff(μ_B)	θ(K)	S	Curie temp.
0.05	3.44×10^{-9}	3.67	72.3	1.40	106K
0.10	1.02×10^{-7}	3.75	84.8	1.44	103K
0.15	1.36×10^{-7}	4.30	94.3	1.71	106K
0.20	4.50×10^{-7}	3.95	96.6	1.54	109K
0.25	2.69×10^{-6}	2.62	68.5	0.90	109K
0.30	3.81×10^{-6}	2.05	64.5	0.64	106K
0.40	6.60×10^{-6}	1.59	64.4	0.44	104K

In the $ThCr_2Si_2$-type structure the metal (M) atoms at Cr sites are tetrahedrally coordinated by Se atoms. In such a situation the energy level of t_{2g} of M is higher than e_g. Based on the observed values of S, ionic states of Mn in the high spin state were estimated to be Mn^{4+} for $0.05 \le x \le 0.20$, Mn^{5+} for x = 0.25 and Mn^{6+} for x = 0.30 and 0.40. In these cases, however, a quite large amount of negative charge is needed to compensate the excess positive charge.

In the case of low spin state, the valence of Mn is assumed to be 0 for $0.05 \le x \le 0.20$, +1 for x = 0.25 and +2 for x = 0.30 and 0.40. These values are much acceptable from the view point of charge neutrality. But, it is suspicious that the valence of Mn is 0 for $0.05 \le x \le 0.20$. It is not clear which spin state is realized in this system.

3.2. $Tl(Cu_{1-x}Fe_x)_2Se_2$ system

Figure 5 shows XRD patterns of $Tl(Cu_{1-x}Fe_x)_2Se_2$ ($0 \le x \le 1$). All obtained samples showed the

$ThCr_2Si_2$-type structure. The observed lattice parameters of $TlCu_2Se_2$ and $TlFe_2Se_2$ were both well compatible with those in the earlier reports[7,8].

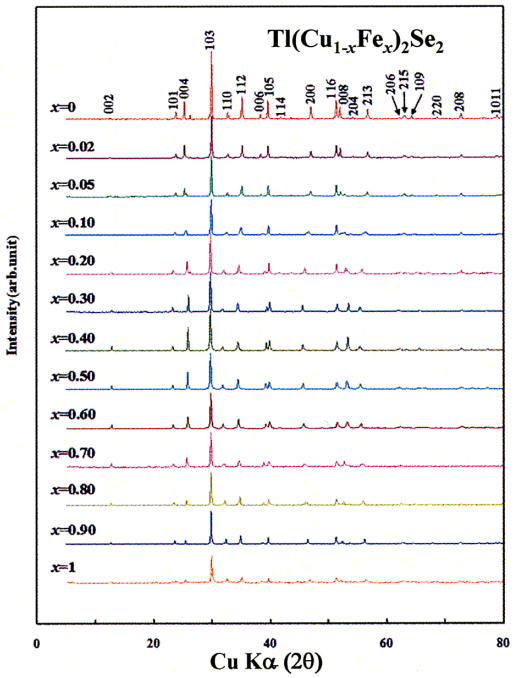

Figure 5. XRD patterns of $Tl(Cu_{1-x}Fe_x)_2Se_2$ ($0 \le x \le 1$).

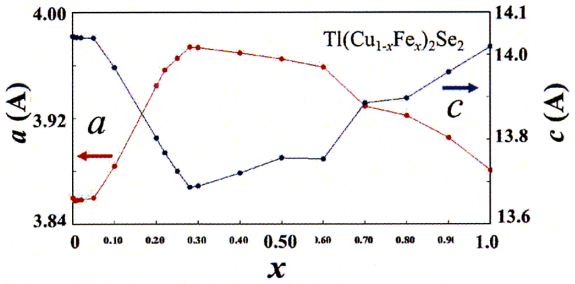

Figure 6. Lattice parameters of $Tl(Cu_{1-x}Fe_x)_2Se_2$ ($0 \le x \le 1$) as a function of x.

Figure 6 shows the lattice parameters of $Tl(Cu_{1-x}Fe_x)_2Se_2$ ($0 \le x \le 1$) as a function of x. In spite of that $TlCu_2Se_2$ and $TlFe_2Se_2$ have the same crystal structure to each other, the lattice parameters do not obey a Vegard's rule, exhibiting a maximum in the a parameter and a minimum in the c parameter at x = 0.26. Berger and Van Bruggen observed similar sharp bends in the lattice parameters at x = 0.25[17]. It was reported that $TlCu_{1.5}Fe_{0.5}Se_2$ [$Tl(Cu_{0.75}Fe_{0.25})_2Se_2$] is a new mineral (bukovite) with the $ThCr_2Si_2$-type structure[19,20]. The lattice constants of the present samples of x = 0.25-0.30 are well consistent with the values of the bukovite[19, 20]. There would be a lattice ordering or a charge ordering in this mineral. It should be noted that in the composition of x = 0.25 all iron atoms would have the oxidation state of Fe^{3+}, with the copper atoms being in the state of Cu^{+}. This figure suggests the existence of another phase at x = 0.05. There is no report on this phase. An atomic ordered structure would exist at this composition. In addition, another new phase may exist at x = 0.60-0.70, although uncertain.

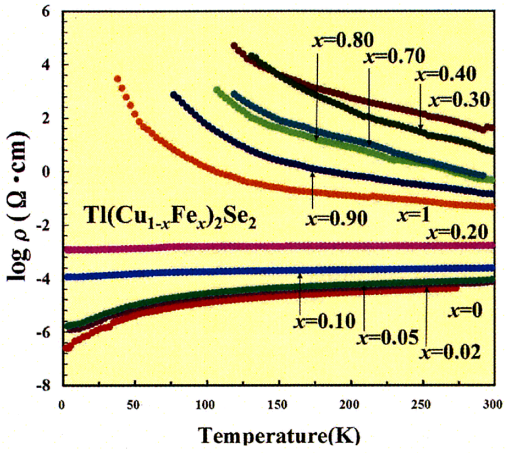

Figure 7. Temperature variations of electrical resistivity ρ of $Tl(Cu_{1-x}Fe_x)_2Se_2$ ($0 \le x \le 1$).

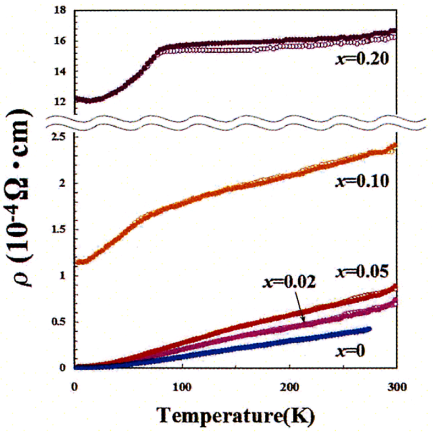

Figure 8. Temperature variations of electrical resistivity ρ of $Tl(Cu_{1-x}Fe_x)_2Se_2$ ($0 \le x \le 0.10$).

Figure 7 shows temperature variations of $\log\rho$ of $Tl(Cu_{1-x}Fe_x)_2Se_2$ ($0 \le x \le 1$). In the range of $x \le 0.20$ the samples show the metallic conduction; the resistivity increases with increasing x. This tendency can

be explained by that the substituted Fe has the higher valence state than Cu, resulting in the decrease of the hole number. In the range of $x \geq 0.30$, samples showed semiconductive conduction. The resistivity decreases with increasing x, which may be due to the contraction of a axis, because the conduction is mainly carried out in the a-b planes. The energy gap Eg also decreases with increasing x: e.g. Eg = 0.09 eV and 0.03 eV for x = 0.30 and 1.0, respectively. These values are somewhat smaller than those of earlier reports[8, 17]. As shown in Fig. 8, ρ–T curves for x = 0.10 and 0.20 showed sharp drops at ~70 and ~80 K, respectively. Open circles and closed circles indicate the results obtained in the cooling run and subsequent heating run, respectively. The hysteresis was observed in the sample of x = 0.20. These anomalies are attributed to ferromagnetic ordering, that will be described below.

Figure 9 gives $(\rho - \rho_0)$ as a function of T^2 for the samples of $Tl(Cu_{1-x}Fe_x)_2Se_2$ (x = 0, 0.02, and 0.05), where ρ_0 is residual resistivity. The values of $(\rho - \rho_0)$ show a linear dependence to T^2 below about 25 K for all samples. The coefficients of gradient are estimated to be, $1.41\times10^{-9}\ \Omega\cdot cm\cdot K^{-2}$, $2.21\times10^{-9}\ \Omega\cdot cm\cdot K^{-2}$, and $3.31\times10^{-9}\ \Omega\cdot cm\cdot K^{-2}$ for x = 0, 0.02, and 0.05, respectively. These values are much larger than those of ferromagnetic metals of Fe and Ni metals ($\sim1.0\times10^{-11}\ \Omega\cdot cm\cdot K^{-2}$), suggesting the existence of strong electron correlation in these compounds.

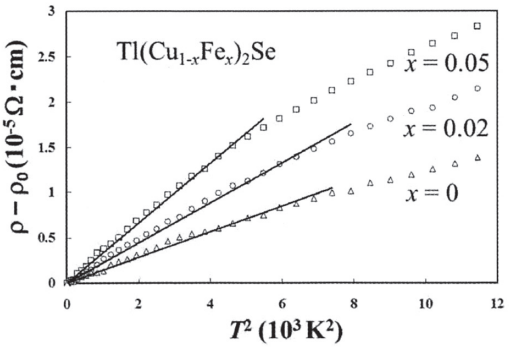

Figure 9. The resistivity $(\rho - \rho_0)$ as a function of T^2 of $Tl(Cu_{1-x}Fe_x)_2Se_2$, where ρ_0 is residual resistivity.

Figure 10 shows temperature variations of Seebeck coefficients S of $Tl(Cu_{1-x}Fe_x)_2Se_2$. The values of S were positive for the samples $x \leq 0.27$, and negative for $x \geq 0.29$, showing that the dominant carriers are holes for the former samples and electrons for the latter samples. These results are consistent with the observations of the change of physical properties near x = 0.25-0.30 mentioned above, suggesting the existence of bukovite at this composition.

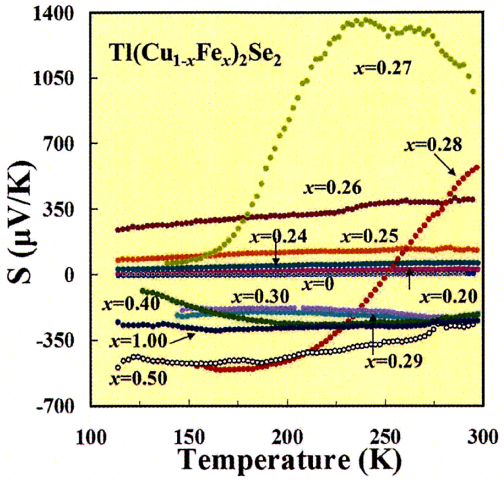

Figure 10. Temperature variations of Seebeck coefficients S of $Tl(Cu_{1-x}Fe_x)_2Se_2$ ($0 \leq x \leq 1$).

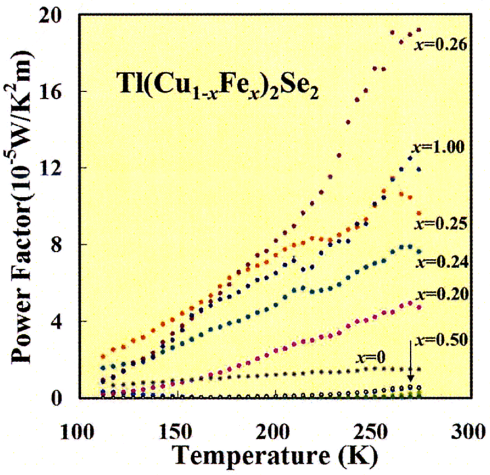

Figure 11. Temperature variations of thermoelectric power factor (S^2/ρ) of $Tl(Cu_{1-x}Fe_x)_2Se_2$ ($0 \leq x \leq 1$).

Figure 11 exhibits temperature variations of thermoelectric power factor (S^2/ρ) of $Tl(Cu_{1-x}Fe_x)_2Se_2$ ($0 \leq x \leq 1$). The values of power factor increase with increasing temperature for each sample. Much larger values of S are expected in the higher temperature range above 300 K. Power factors observed at 273 K are plotted in Fig. 12 as a function of x. Samples of $0.25 \leq x \leq 0.28$ and x =1.0 have relatively higher values of power factor (= ~ 10^{-4} $WK^{-2}m^{-1}$).

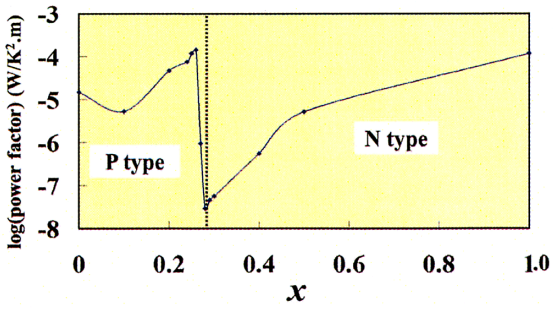

Figure 12. Thermoelectric power factor of $Tl(Cu_{1-x}Fe_x)_2Se_2$ ($0 \le x \le 1$) observed at 273 K as a function of x.

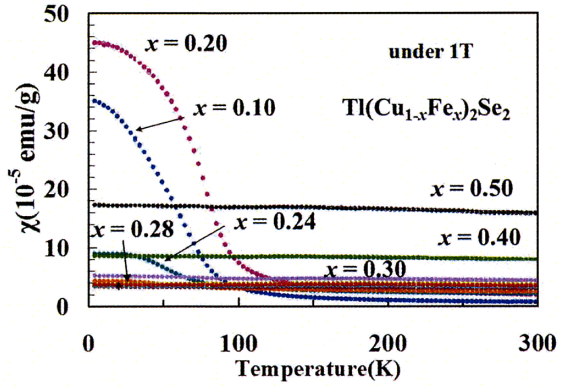

Figure 13. Temperature variations of the magnetic susceptibility χ of $Tl(Cu_{1-x}Fe_x)_2Se_2$ measured under 1T.

Figure 13 shows temperature variations of the magnetic susceptibility χ of $Tl(Cu_{1-x}Fe_x)_2Se_2$ measured under 1T. Samples of $0.10 \le x \le 0.24$ showed the ferromagnetic transition. The Curie temperature slightly increases with x from ca.70 K and ca.80 K for x = 0.005 and 0.20, respectively. Above the Curie temperature the values of χ obeyed a Curie-Weiss law $\chi = \chi_0 + C/(T - \theta)$. Values of θ were observed to be positive, consistent with the observation of Curie temperature. The observed effective Bohr magnetons showed that the total spin angular momentum S for one Fe ion is about 5/2. Since Cu^+ have no localized moment, the observed magnetic moments originate from the iron ions. These results suggest that the ionic state of the substituted Fe is Fe^{3+}.

We found that the samples of $x \ge 0.28$ showed the ferromagnetism in χ measurements up to 500 K, above which temperature samples showed a broad maximum of χ possibly due to an incongruent melting. Although no impurity phase was observed in the XRD patterns, the coexistence of magnetic impurities such as Fe_3O_4 cannot be excluded.

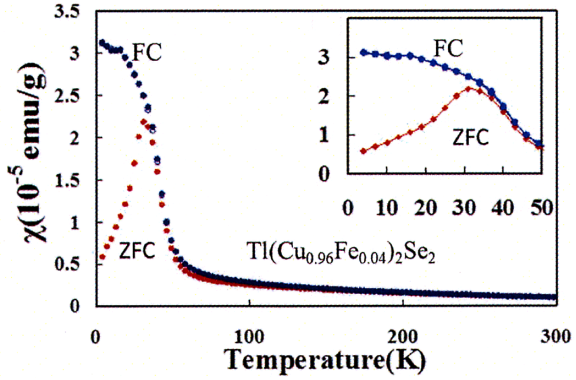

Figure 14. Temperature variations of χ of the sample of $Tl(Cu_{0.96}Fe_{0.04})_2Se_2$ observed in cooling-heating runs under 0.02 T (FC), and measured on heating under 0.02T after zero field cooling (ZFC). The inset is the enlarged figure below 50 K.

It was reported that the magnetic interaction of $Tl(Cu_{1-x}Fe_x)_2Se_2$ in the composition of $x \le 0.25$ can be explained by the mictomagnetiasm consisting with a RKKY (Ruderman-Kittel-Kasuya-Yoshida) interaction and a superexchange interaction[17]. Figure 14 exhibits temperature variations of χ of the sample of x = 0.04 observed in cooling-heating runs under 0.02T, and measured on heating under 0.02T after zero-field cooling. The temperature dependence of χ measured after field-cooling showed the Curie temperature at ca.70K. On the other hand, the χ-T curve obtained by zero-field cooling showed a cusp at ca. 20K, which is characteristic of the spin glass[21]. These results clearly show that two types of magnetic interactions are coexisting in this sample: the long range magnetic interaction and the spin glass. These mictomagnetic behaviors are substantially same as the mechanism mentioned above[17]. The spin-glass like behavior is usually observed in metallic compounds with a small amount of magnetic impurities.

3.3. $Tl(Cu_{1-x}Co_x)_2Se_2$ system

$TlCo_2Se_2$ has the $ThCr_2Si_2$-type structure[22]. Figure 15 shows lattice parameters of $Tl(Cu_{1-x}Co_x)_2Se_2$ as a function of x. The lattice parameters show somewhat complicated dependence on x. Both a and c change continuously with x in a range $0 \le x \le 0.3$, indicating that a new phase exists at x = 0.30. The figure suggests the existence of another new phase at x = 0.60 and 0.90. These phases would have the modified

$ThCr_2Si_2$-type structure. The notable is that the XRD pattern of the sample of $x = 0.50$ showed the coexistence of two phases having the $ThCr_2Si_2$-type structure with different lattice parameters; the difference of parameters is more remarkable in a. These results were quite reproducible. But, the origin is not clear.

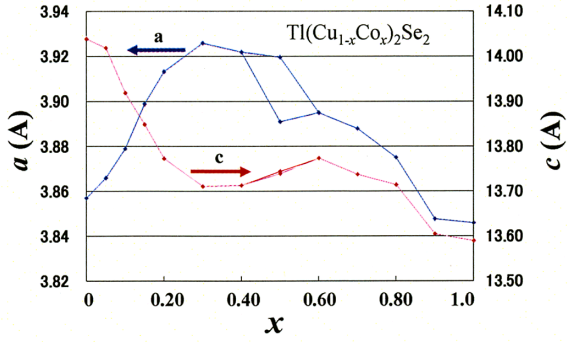

Figure 15. Lattice parameters of $Tl(Cu_{1-x}Co_x)_2Se_2$ ($0 \le x \le 1$) as a function of x.

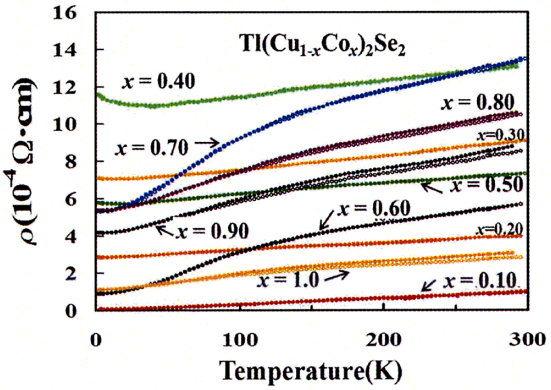

Figure 16. Temperature variations of electrical resistivity ρ of $Tl(Cu_{1-x}Co_x)_2Se_2$ ($0 \le x \le 1$).

Figure 16 exhibits temperature variations of ρ of $Tl(Cu_{1-x}Co_x)_2Se_2$ ($0 \le x \le 1$). All samples show metallic behavior. The resistivity increases with x up to 0.40, and shows the decreasing tendency from $x = 0.5$ to 0.6. The resistivity increases again at $x = 0.7$, and then decreases with x up to $x = 1.0$. The curves are concave upward in the samples of $0.60 \le x \le 0.90$, which may correspond to the ferromagnetic ordering.

Figure 17 shows temperature variations of magnetic susceptibility χ of $Tl(Cu_{1-x}Co_x)_2Se_2$ from 4 to 300 K. Ferromagnetic transition was observed in the samples of $x \ge 0.40$. Figure 18 shows the enlarged figures of χ of $Tl(Cu_{1-x}Co_x)_2Se_2$ samples for $0.10 \le x \le 0.60$.

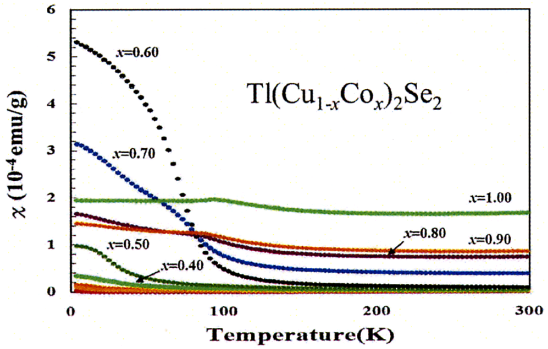

Figure 17. Temperature variations of magnetic susceptibility χ of $Tl(Cu_{1-x}Co_x)_2Se_2$ ($0 \le x \le 1$) measured under 1T.

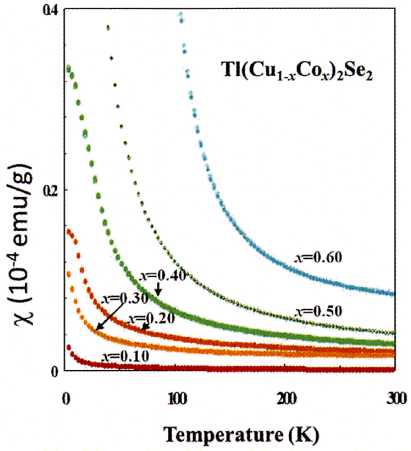

Figure 18. Temperature variations of χ of $Tl(Cu_{1-x}Co_x)_2Se_2$ ($0.10 \le x \le 0.60$) measured under 1 T.

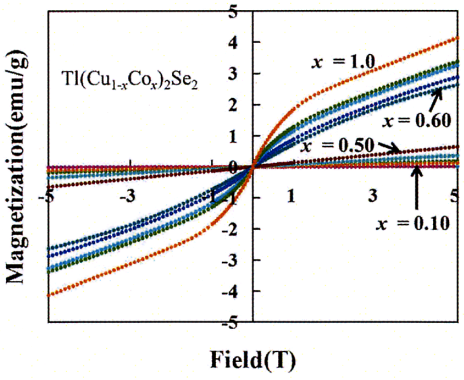

Figure 19. Magnetization curves of $Tl(Cu_{1-x}Co_x)_2Se_2$ ($0.10 \le x \le 1$) measured at 90 K.

Figure 19 gives magnetization curves of the samples of $0.10 \le x \le 1.0$ measured at 90 K. The samples of $x \ge 0.60$ show small magnetic hysteresis curves, indicating that the samples are ferromagnetic at this temperature. The samples of $x \le 0.50$ show the paramag-

netic behaviors.

Above the Curie temperature magnetic susceptibility obeyed Curie-Weiss law, $\chi = \chi_0 + C/(T - \theta)$. Calculated magnetic parameters of $Tl(Cu_{1-x}Co_x)_2Se_2$ are listed in Table II. The values of Weiss constant θ are negative for $x \leq 0.30$ and positive for $0.40 \leq x \leq 1$, indicating that the magnetic exchange interaction is antiferromagnetic and ferromagnetic for the former and the latter, respectively. The positive values of θ for $0.40 \leq x \leq 1$ are well consistent with the observation of ferromagnetic transition. The ferromagnetism would be intrinsic to these compounds, because the possibly coexisting impurity phase of $CoSe_2$ is a paramagnet[23].

Table II. Magnetic parameters of $Tl(Cu_{1-x}Co_x)_2Se_2$. P_{eff} is effective Bohr magneton. θ is Weiss temperature. S is total spin angular momentum,

composition x	χ_0(emu/g)	Peff(μ_B)	θ(K)	S	Curie temp.
0.05	2.65×10^{-8}	2.46	-23.8	0.83	
0.10	1.42×10^{-7}	0.98	-41.7	0.20	
0.20	8.75×10^{-7}	1.90	-37.8	0.58	
0.30	1.18×10^{-6}	0.84	-24.8	0.15	
0.40	9.59×10^{-7}	1.64	1.88	0.16	22K
0.50	1.07×10^{-6}	1.83	20.0	0.54	25K
0.60	5.16×10^{-4}	1.61	81.7	0.45	100K
0.70	3.23×10^{-5}	1.65	81.8	0.46	94K
0.80	6.69×10^{-5}	1.41	86.9	0.37	94K
0.90	7.50×10^{-4}	1.87	60.4	0.56	97K
1.00	1.54×10^{-5}	1.60	77.0	0.44	112K

3.4. $TlCo_{2-x}Se_2$ system

$TlCo_{2-x}Se_2$ ($0 \leq x \leq 0.10$) showed the $ThCr_2Si_2$-type structure. Lattice parameters were observed to be a = 0.3844 nm and c = 1.359 nm for x = 0, well consistent with the reference values[22]. The lattice parameters were scarcely changed with x.

Figure 20 shows temperature variations of electrical resistivity ρ of $TlCo_{2-x}Se_2$ (x = 0 and 0.10). Both samples show the metallic behavior. The thermal hysteresis was observed above about 70 K for both samples, suggesting the existence of first order phase transition.

Figure 21 shows temperature variations of magnetic susceptibility χ for $TlCo_{2-x}Se_2$ ($0 \leq x \leq 0.10$). The values of χ tend to decrease with increasing x. All samples show a cusp near 100 K, suggesting antiferromagnetic ordering. The transition temperature was 100 K and 80 K for x = 0 and 0.10, respectively. These anomalies are consistent with temperature dependences of ρ in Fig. 20. No thermal hysteresis was observed above the transition in χ measurements.

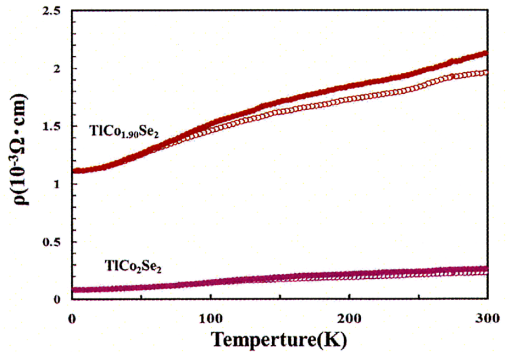

Figure 20. Temperature variations of ρ of $TlCo_{2-x}Se_2$. Measurements were done on cooling (open circles), and subsequently on heating from 2 K (closed circles).

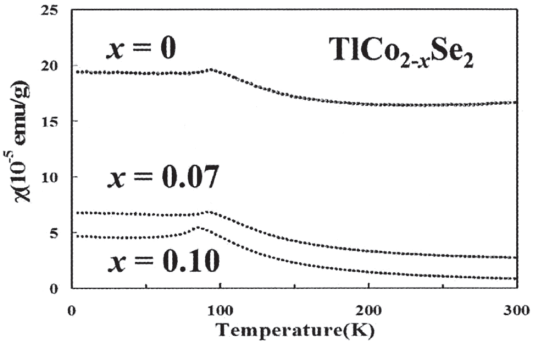

Figure 21. Temperature dependences of χ for $TlCo_{2-x}Se_2$ ($0 \leq x \leq 0.10$) measured under 1 T.

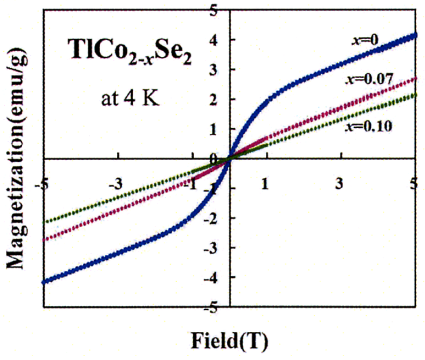

Figure 22. Magnetization curves of $TlCo_{2-x}Se_2$ ($0 \leq x \leq 0.10$) measured at 4 K.

Figure 22 gives the magnetization curves of $TlCo_{2-x}Se_2$ ($0 \leq x \leq 0.10$) measured at 4 K. Samples of x = 0 and 0.07 show the ferromagnetic field dependences, while sample of x = 0.10 shows paramagnetic (or antiferromagnetic) behavior. Ferromag-

netism was also observed for the samples of x = 0, 0.07 at 273 K, suggesting the existence of some ferromagnetic impurity (-ies).

3.5. $Tl(Cu_{1-x}Ni_x)_2Se_2$ system

XRD measurements revealed that Ni can be substituted for Cu up to x = 0.10 of $Tl(Cu_{1-x}Ni_x)_2Se_2$. The parameter a slightly increased with increasing x from 0.3860 nm to 0.3862 nm for x = 0 and 0.10, respectively. The parameter c slightly decreased with increasing x from 1.405 nm to 1.401 nm for x = 0 and 0.10, respectively. Consequently, the ratio of c/a decreased with increasing x.

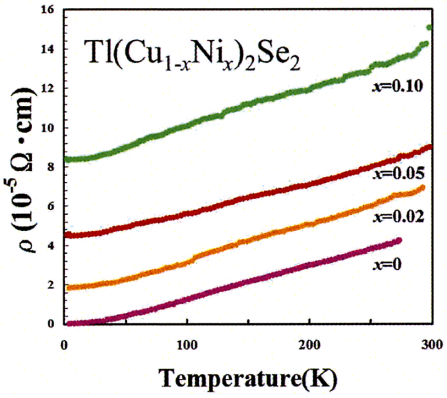

Figure 23. Temperature variations of the resistivity ρ of $Tl(Cu_{1-x}Ni_x)_2Se_2$ ($0 \le x \le 0.10$).

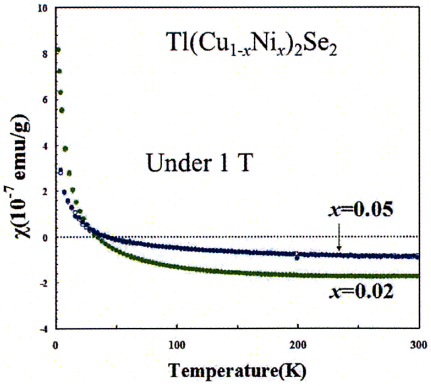

Figure 24. Temperature variations of χ of $Tl(Cu_{1-x}Ni_x)_2Se_2$ (x = 0.02, 0.05) measured under 1 T.

Figure 23 shows the temperature variations of electrical resistivity ρ of $Tl(Cu_{1-x}Ni_x)_2Se_2$ ($0 \le x \le 0.10$). All samples showed the metallic behavior, with the values of ρ increasing as x increases. Figure 24 shows the magnetic susceptibility of $Tl(Cu_{1-x}Ni_x)_2Se_2$ (x = 0.02, 0.05) as a function of temperature. The samples show diamagnetism with a little amount of paramagnetic moments. These behaviors are consistent with the reported results of the Pauli paramagnetic nature of $TlNi_2Se_2$[24].

3.6. $Tl(Cu_{1-x}Ag_x)_2Se_2$ system

XRD patterns for $Tl(Cu_{1-x}Ag_x)_2Se_2$ ($0 \le x \le 0.10$) system showed a small amount of impurity phase of $TlCuSe_2$. We consider, however, that Ag atoms are substituted for Cu atoms, because we notice no silver selenides in these samples. The lattice parameters of both a and c slightly contracted with increasing x.

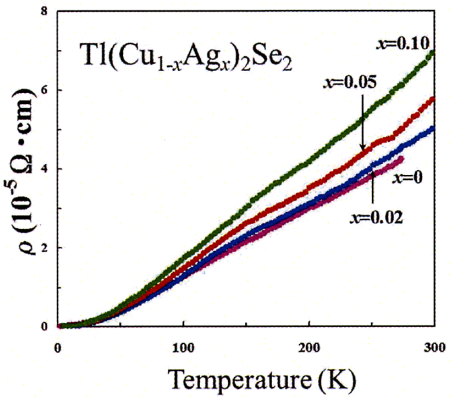

Figure 25. Temperature variations of the electrical resistivity ρ of $Tl(Cu_{1-x}Ag_x)_2Se_2$ ($0 \le x \le 0.10$).

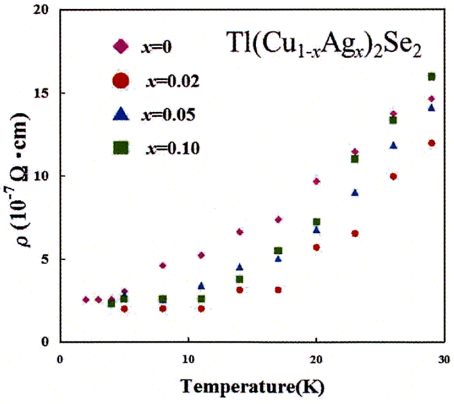

Figure 26. Temperature variations of ρ of $Tl(Cu_{1-x}Ag_x)_2Se_2$ ($0 \le x \le 0.10$) below 30 K.

Figure 25 shows temperature variations of ρ of $Tl(Cu_{1-x}Ag_x)_2Se_2$ ($0 \le x \le 0.10$). The values of ρ slightly increased with increasing x. As mentioned

before, $TlCu_2Se_2$ shows a quite small resistivity at low temperatures[6]. It is interesting that the values of ρ of the Ag-substituted samples are much smaller than that of $TlCu_2Se_2$ below about 30 K as shown in Fig. 26. This is quite unusual, because the substituted Ag atoms would act as a scattering factor causing the increase of ρ. Magnetic susceptibility for these compounds showed diamagnetism with a minority of paramagnetism.

4. Summary

$Tl(Cu_{1-x}Mn_x)_2Se_2$ was found to have $ThCr_2Si_2$-type structure in the range $x \leq 0.40$. $Tl(Cu_{1-x}M_x)_2Se_2$ (M = Fe and Co) showed basically $ThCr_2Si_2$-type structure in the range of $0 \leq x \leq 1$. A new phase with possible modified $ThCr_2Si_2$-type structure was found in $Tl(Cu_{1-x}Fe_x)_2Se_2$ with $x = 0.05$. $Tl(Cu_{1-x}Co_x)_2Se_2$ showed new phases having possibly modified $ThCr_2Si_2$-type structure in the compositions of x = 0.30, 0.60, and 0.90. Ni and Ag were both substituted for Cu up to $x = 0.10$. Samples of $Tl(Cu_{1-x}Mn_x)_2Se_2$ were metallic and ferromagnetic. Curie temperature T_c is ca. 100 K. $Tl(Cu_{1-x}Fe_x)_2Se_2$ showed metallic conduction for $x \leq 0.20$ and semiconductive conduction for $x \geq 0.30$. All samples of this series showed ferromagnetism. $Tl(Cu_{1-x}Co_x)_2Se_2$ showed metallic conductivity. Sample of $x \geq 0.40$ showed ferromagnetism: $T_c = \sim 20$ K for $x = 0.40$ and 0.50, and $T_c = \sim 100$ K for $x \geq 0.60$. $(Cu_{1-x}Ni_x)_2Se_2$ samples showed metallic and diamagnetic behaviors. $(Cu_{1-x}Ag_x)_2Se_2$ samples were diamagnetic metals.

KFe_2Se_2 with $ThCr_2Si_2$ structure was reported to be a new superconductor[25]. The FeSe layers are responsible for the high T_c (~30 K). Present compounds, however, showed no superconductivity above 2 K.

This paper was prepared based on the master's theses for graduate school submitted by T. Morinaga (2007), S. Namba (2009), and S. Nakai (2010).

Acknowledgement

The preset authors greatly thank to Prof. K. Hirota and Prof. M. kato for fruitful discussion on $TlCo_{2-x}Se_2$. The authors are also grateful to Prof. N. Nakayama for useful suggestions on $Tl(Cu_{1-x}Fe_x)_2Se_2$.

References

1) J. C. W. Folmer and F. Jellinek, *J. Less-Common Met.*, **76**, 153 (1980).
2) C. Burschka and W. Bronger, *Z. Natureforsch.*, **32b**, 11 (1977).
3) G. Savelsberg and H. Schafer, *Z. Natureforsch.*, **33b,** 711 (1978).
4) M. Saeki, M. Onoda, and H. Nozaki, *Mater. Res. Bull.*, **23**, 603 (1988).
5) M. Onoda and M. Saeki, *Mater. Res. Bull.*, **24**, 1337 (1989).
6) R. Berger, *J. Less-Common Met.*, **147**, 141 (1989).
7) K. O. Klepp and H. Boller, *Monatsh. Chem.*, **109**, 1049 (1978).
8) G. Brun, B. Gardes, J. C. Tedenac, A. Raymond, and M. Maurin, *Mater. Res. Bull.*, **14**, 743 (1979).
9) R. Berger, and C. F. Van Bruggen, *J. Less-Common Met.,* **99**, 113 (1984).
10) K.O. Klepp, H. Boller, and H. Vollenkle, *Monatsh. Chem.,* **111**, 727 (1980).
11) T. Ohtani, J. Ogura, M. Sakai, and Y. Sano, *Solid State Commun.*, **78**, 913 (1991).
12) T. Ohtani, J. Ogura, H. Yoshihara, and Y. Yokota, *J. Solid State Chem.*, **115**, 379 (1995).
13) T. Ohtani, T. Hoshino, A. Tsujinouchi, and M. Hasegawa, *Mater. Res. Bull.*, **30**, 161 (1995).
14) T. Ohtani, T. Hoshino, S. Tanaka, Y. Okada, N. Nagaoka, and Y. Yokota, *Crys. Res. Technol.*, **31**, 865 (1996).
15) T. Ohtani, H. Takeuchi, K. Koh, and T. Kaneko, *J. Alloys Comp.*, **317-318**, 201 (2001).
16) T. Ohtani M. Taniguchi, S. Sasaki, H. Kishi, and T. Nakata, *J. Alloys Comp.*, **383**, 245 (2004).
17) R. Berger, and C. F. Van Bruggen, *J. Less-Common Met.*, **113**, 291 (1985).
18) B. Raveau and M. M. Seikh, *Handbook of Mag. Mater.* **23**, 161 (2015).
19) Z. Johan and M. Kvacek, *Bull. Soc. Fr. Mineral. Cristallogr.*, **94**, 529 (1971).
20) J. C. Tedenac, G. Brun, B. Gardes, S. Peytavin, and M. Maurin, *C. R. Acad. Sci., Paris,.Ser. C,* **283**, 529 (1976).
21) K. H. Fischer and J. A. Hertz, "Spin Glasses", Cambridge University Press (1991).
22) JCPDF (File No. 79-2121).
23) K. Adachi, M. Matsui, and M. Kawai, *J. Phys. Soc. Jpn.*, **46**, 1474 (1979).
24) A.R. Newmark, G. Huan, M. Greenblatt, and M. Croft, *Solid State Commun.*, **71**, 1025 (1989).
25) J. Guo, S. Jin, G. Wang, S. Wang, K. Zhu, T. Zhou, M. He, and X. Chen, *Phys. Rev. B,* **82**, 180520 (R) (2010).